Applied Microscopy
Korean Society of Microscopy
pISSN 2287-5123 · eISSN 2287-4445
http://dx.doi.org/10.9729/AM.2013.43.3.122

Direct Observation of Heterogeneous Nucleation in Al-Si-Cu-Mg Alloy Using Transmission Electron Microscopy and Three-dimensional Atom Probe Tomography

Jun Yeon Hwang*, Rajarshi Banerjee[1], David R. Diercks[2], Michael J. Kaufman[2]

Institute of Advanced Composite Materials, Korea Institute of Science and Technology, Jeollabuk-do 565-905, Korea
[1]Center for Advanced Research and Technology, University of North Texas, Denton, TX 76207, USA
[2]Department of Metallurgical and Materials Engineering, Colorado School of Mines, Golden, CO 80401, USA

*Correspondence to:
Hwang JY,
Tel: +82-63-219-8144
Fax: +82-63-219-8419
E-mail: Junyeon.Hwang@kist.re.kr

Received September 12, 2013
Revised September 26, 2013
Accepted September 26, 2013

The heterogeneous nucleation of the θ' phase on nanoscale precipitates has been investigated using a combination of three-dimensional atom probe tomography and high-resolution transmission electron microscopy. Two types of θ' phases were observed, namely small (~2 nm thick) cylindrical precipitates and larger (~100 nm) globular precipitates and both appear to be heterogeneously nucleated on the nanoscale precipitates. The composition and crystal structure of precipitates were directly analyzed by combination of two advanced characterization techniques.

Key Words: Transmission electron microscopy, Atom probe tomography, Precipitate, Heterogeneous nucleation

INTRODUCTION

Three-dimensional atom probe (3DAP) tomography combined with high resolution transmission electron microscopy (TEM) techniques have given the atomic scale resolution in the materials characterization. The advent of these advanced characterization leads the new science and uncover the question in the atomic behavior in material characterization. Precipitation strengthening mechanisms and precipitation kinetics have become the subject of much research since the discovery of Guinier-Preston (GP) zones (Guinier, 1938; Preston, 1938). In the case of Al-Cu alloys, it is now well accepted that the sequence of precipitation can be summarized as: solid solution → GP zones → metastable θ" → metastable θ' → stable θ (Al_2Cu). The GP zones and the metastable θ" and θ' phases have been shown to be the primary strengthening phases. Thus, the examination of GP zones and the metastable phases, are important during the aging process not only for process control but also for understanding the fundamentals aspects of the precipitation sequences and their relation to strengthening mechanisms (Fujita & Lu, 1992). Over the past several decades, there have been numerous studies that attempt to reveal the microstructural evolution of the GP zone structures, from nucleation to transformation of the GP structure to the equilibrium Al_2Cu phase. Due to the small size of these features, TEM has been the primary tool used to examine the nature of these nanoscale precipitates (Konno et al., 2001). However, TEM is basically a two-dimensional technique which makes it difficult to observe the full 3D structure and composition of nanoscale precipitates.

To date, there are tremendous efforts have been focused to develop advanced aluminum alloys for in order to satisfy various demands of engineering fields. Among the many commercial engineering aluminum alloys, the quaternary Al-Si-Cu-Mg system has been examined recently because these alloys exhibit high strength and ductility as well as enhanced thermal stability (Martin, 1980; Hutchinson & Ringer, 2000).

The precipitation sequence in these quaternary alloys is rather complex and involves several different metastable and/or stable phases as dominant hardening phases (Eskin, 2003). Thus, understanding the nucleation mechanisms and sequences are important subjects for optimizing alloy design and process development in this system.

Based on general nucleation theory, the GP structure develops homogeneously from solid solution during the early stages of the aging process even though excess vacancies play an important role in the GP formation below the GP zone solvus temperature. Consequently, the θ' phase may develop from transformation of the GP structure in order to minimize free energy during the precipitation sequence. However, if the aging is carried out above the θ" solvus temperature, the θ' phase will be heterogeneously nucleated preferentially on dislocations. Likewise, θ nucleates and grows at grain boundaries above the θ' solvus temperature. In addition, there are also some reports on the continuous transformation of GP zones into θ", then into the θ' phase with increasing thickness (Hwang et al., 2009). To date, there have been few reports of the heterogeneous nucleation of θ' precipitates from the precursor GP zones or assisted by other types of precipitates. The difficulty of direct observation of such effects is due to the extremely small size of the precursor and product phases and the inability to detect this reaction. The recent development of 3DAP tomography can now be combined with high-resolution TEM allowing for the observation of atomic-scale nucleation of precipitates. With electron microscopy providing the capability of structural determination, applying the two techniques together leads to more comprehensive results including both structural and chemical information.

In this study, the heterogeneous nucleation of two different morphologies of θ' phases, from two different particle-associated nucleation sites was found as metastable precursors of the quaternary Al-Mg-Si-Cu phase and Mn containing particles. Based on the results, a nucleation mechanism of the θ' precipitate is discussed.

MATERIALS AND METHODS

The alloy used in this experiment is Al-1.1Si-2.0Cu-0.5Mg-0.5Fe-0.6Mn (in wt. %). Two step heat treatment was performed after solution heat treatment at 488°C for 8 hours. First low temperature at 193°C for 8 hours and then high temperature at 223°C for 4 hours was conducted for stabilizing treatment (T7). The microstructures of the overaged samples were examined by high resolution TEM using an FEI Tecnai F20 (FEI Corp., Hillsboro, OR, USA) equipped with energy dispersive X-ray spectroscopy. For observation with Z-contrast generated by high angle annular dark field, scanning TEM was used. The thin foil specimens for TEM analysis were prepared using a twin-jet electropolishing unit in a 33% nitric acid-methanol solution at –20°C. Before the TEM observations, plasma cleaning was carried out on the thin foil specimens to prevent artifacts from surface contamination.

The 3DAP analysis was performed using a local electrode atom probe (LEAP) 3000X system from Cameca (Madison, WI, USA). The sharp needle specimens for the atom probe analysis were prepared using a FEI Nova 200 (FEI Corp.) dual beam focused ion beam/scanning electron microscope (FIB/SEM). After aging the sample, representative matrix dendritic regions were selected for milling using the FIB, and then lifted out using a nanomanipulator and attached to Si microtip posts. One lift-out region was used to make several specimens as has been previously reported (Miller & Russell, 2007; Thompson et al., 2007). Initial thinning of the material was carried out with a 30 kV ion beam. Final sample cleaning was performed with a 5 kV ion beam to reduce the depth of gallium implantation and surface damage to the LEAP specimens. The final specimens prepared by FIB have ~60 nm tip radii; these were examined initially by TEM and then by 3DAP in an effort to generate accurate structure and compositional information.

RESULTS AND DISCUSSION

Due to the complexity of the various alloying elements, the identification of each metastable phase during aging was not attempted. Unfortunately, the details of microstructural evolution of this alloy are not clearly understood. A typical microstructure (Fig. 1) contains the θ' phase as "plates" with dimensions of 3~5 nm thickness and 80~120 nm length and

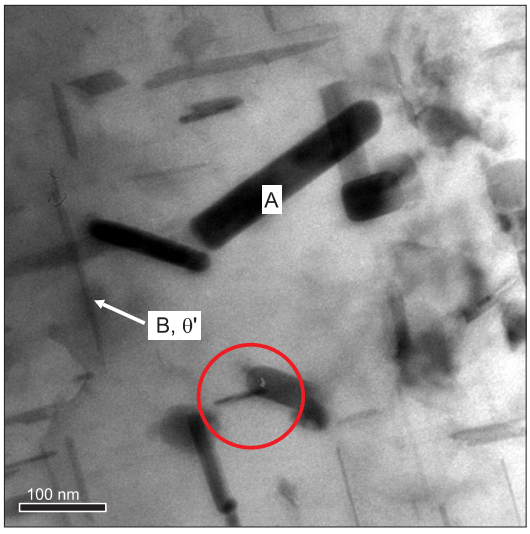

Fig. 1. Transmission electron microscopy image showing two different precipitates (A and B). The evidence of the heterogeneous nucleation site of the particles were marked in the circle.

width. However, abnormally-thick θ' particles (marked A) were observed occasionally. Based on observations at different tilts, the precipitate marked by A appears to have a lath-like morphology, while the precipitate marked B appears to have a plate-like morphology. 3DAP analysis of this material also revealed supporting evidence for the existence of two different morphologies of the Cu-containing precipitates. It is very interesting to find a lath-like Al_2Cu precipitate with an orientation relationship with the matrix. Generally, Al_2Cu are known as a primary hardening phases in this system (Hono et al., 1993). One is the common θ' phase lying along the $\{100\}_{Al}$ planes and the other is the Ω phase which are also plates that lie along the $\{111\}_{Al}$ planes. They have different habit planes, nucleation mechanisms, and crystal structures, but morphologically they are similar.

Interestingly, it is common to find Mn-containing particles at the ends of these lath-type Al_2Cu precipitates. The bright field TEM image and microdiffraction pattern in Fig. 2 confirm that this globular phase is α-Al[Si,Mn]Cu having cubic structure with lattice parameter of ~1.25 nm. Microdiffraction patterns from the lath-type Al_2Cu phase that nucleated on the globular α-Al[Si,Mn]Cu particle indicate that these laths have the same lattice parameters as the tetragonal θ'-Al_2Cu phase (a=0.4 nm, c=0.58 nm). The high resolution TEM (HRTEM) micrograph and fast Fourier transform (FFT) obtained from a lath-type θ' precipitate (Fig. 3) revealed that this particle has a different orientation relationship with the Al matrix than the typical plate-like θ' phase. The sharp spot near the $(020)_{Al}$ corresponds to $(011)_{\theta'}$, and the spot lying near the forbidden $(210)_{Al}$ location corresponds to $(103)_{\theta'}$. These data suggest that the orientation relationship between the lath-type θ' and the Al matrix is $<311>_{\theta'}//<001>_{Al}$ and $\{011\}_{\theta'}//\{010\}_{Al}$. This is different from the typical orientation relationship of plate-like θ' precipitates with a $\{001\}_{Al}$ habit planes which is $<100>_{\theta'}//<100>_{Al}$ and $\{011\}_{\theta'}//\{001\}_{Al}$. It is believed that the lath shape θ' precipitates nucleate heterogeneously at the edge of the α-Al[Si,Mn]Cu particle particles and grow and thicken losing their coherency with the matrix. Thus, it appears that, for heterogeneous nucleation of θ' from the globular α precipitates, it is not necessary to satisfy the conventional orientation relationship. One interesting report on the effects of Mn-containing dispersoids, i.e., the $Al_{20}Cu_2Mn_3$ phase, which act as heterogeneous nucleation sites for the hexagonal plate shaped Ω phase (Al_2Cu) and the cuboidal σ phase ($Al_5Cu_6Mg_2$) (Mukhopadhyay, 2002). Mukhopadhyya suggested that these Mn-containing particles are predominant nucleation sites for the Ω phase which is a major hardening phase in these systems. However, the number density of the α-Al[Si,Mn]Cu particles is very small in our system, thus it is hard to observe the lath-type θ' phase. Further, there is a small amount of Mn in the primary α aluminum phase, because the Mn partitions with iron to the interdendritic regions during solidification. The solubility of manganese and iron in this system is very low; thus, the manganese is not likely to play a dominant role in the heterogeneous nucleation of the θ' phase.

Another type of heterogeneous nucleation of θ' assisted by cylindrical precipitates containing quaternary Al-Si-Cu-Mg precipitates was also examined. Fig. 4 displays 3DAP results showing the plate-shaped θ' precipitates nucleated on the cylindrical type precipitates. Both the cylindrical precipitate and plate-shaped θ' precipitates are aligned along the same $<001>_{Al}$ direction in the Al matrix as pointed out previously.

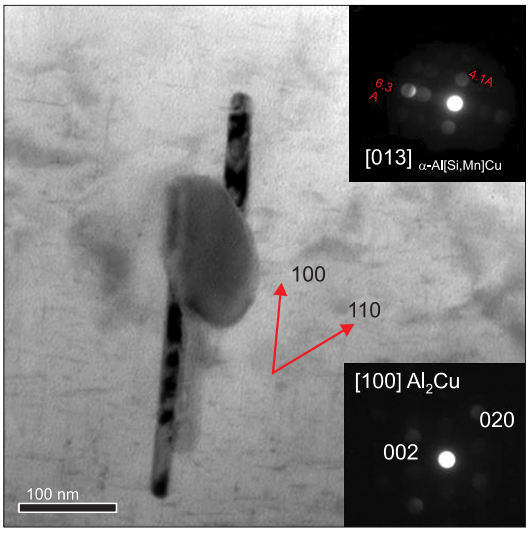

Fig. 2. Bright field transmission electron microscopy image and corresponding micro-diffraction pattern (indexed as a [013] zone axis from α-Al[Si,Mn]Cu) of a region containing the globular phase nucleating two different Al_2Cu laths and micro-diffraction pattern of θ' precipitate.

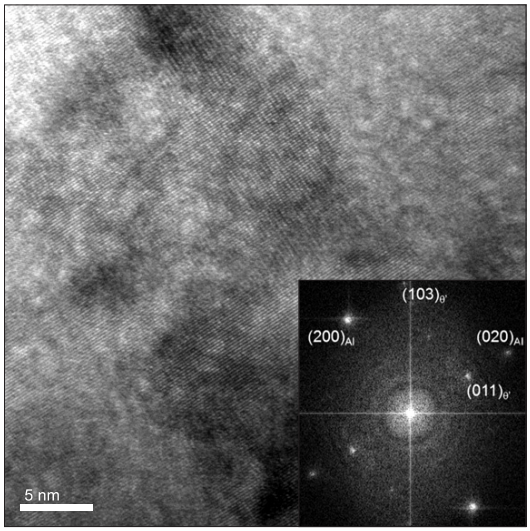

Fig. 3. High resolution transmission electron microscopy image and fast Fourier transform in a inset from a lath-type Al_2Cu precipitate.

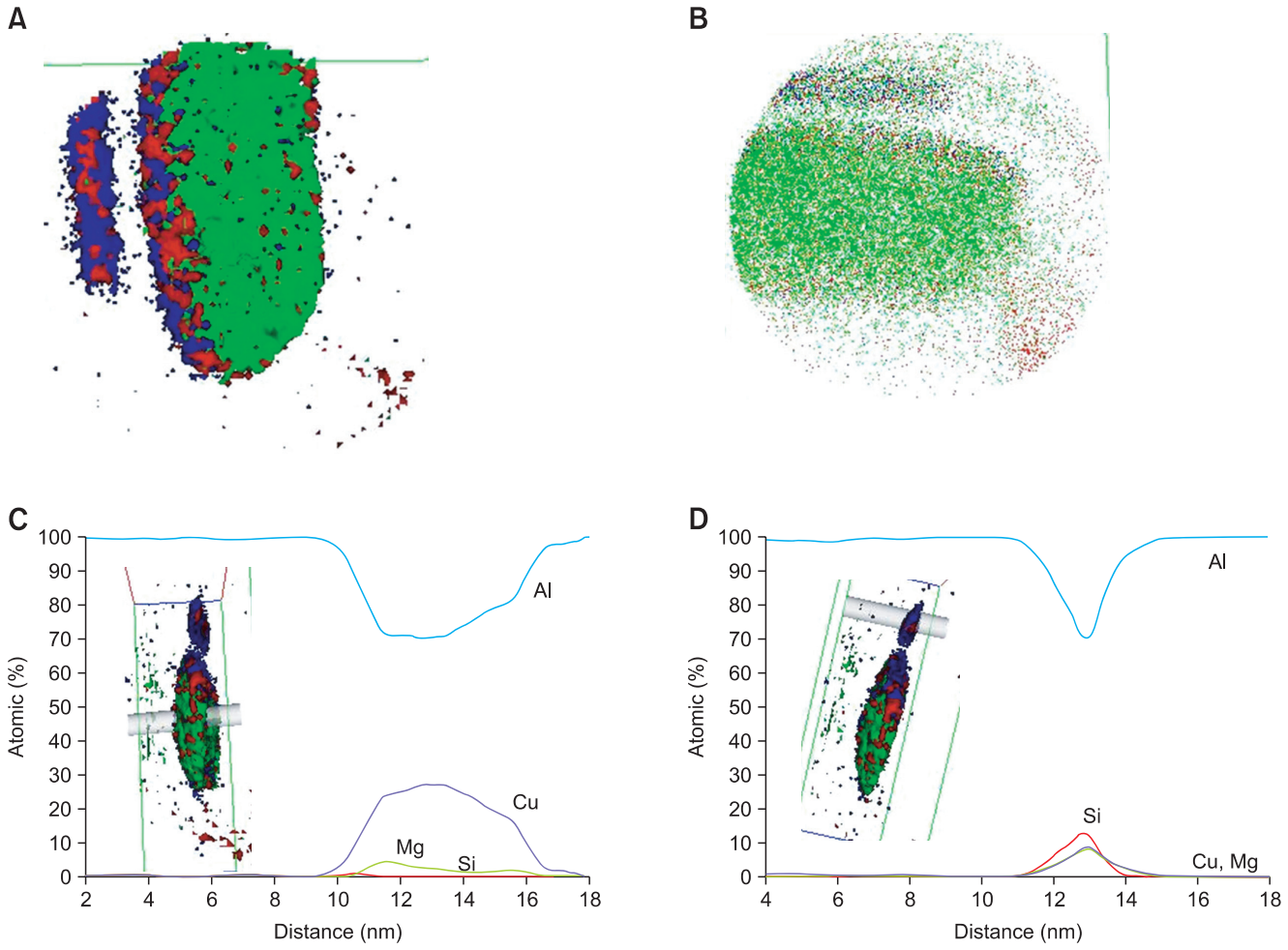

Fig. 4. Three-dimensional atom probe results showing the plate shape of the θ' precipitate that heterogeneously nucleated on the Si modified GPB zone, represented by (A) isoconcentration surface of each atoms, and (B) atomic map; Cu in green, Si in red, and Mg in blue color, respectively. (C and D) Represents the 1 dimensional chemical compositional profile results along the gray cylindrical tube having a 2 nm diameter.

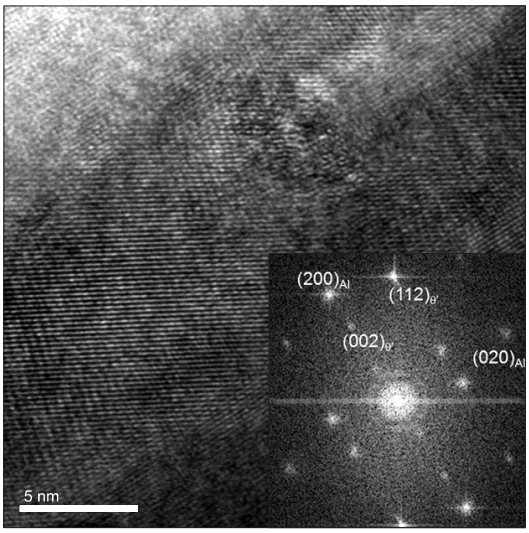

Fig. 5. Bright field transmission electron microscopy image and fast Fourier transform in a inset showing heterogeneous nucleation of the θ' precipitate from the Si-modified GPB zone.

The growth of the plate-shaped θ' precipitate on the heterogeneous nucleation site is likely to follow the general growth mechanism (Hwang, 2009). The θ' particle nucleated along the elongated side of the cylindrical precipitate and grew in the elastically-soft <100> direction in the aluminum matrix. The HRTEM micrograph (Fig. 5) taken from the circled area in Fig. 1 shows that one cylindrical precipitate served as two θ' nucleation sites. The FFT spectra in a inset in Fig. 5 representing the combined θ' and cylindrical precipitate show very complex results. The spots in the FFT spectra corresponding to the cylindrical precipitate are unclear, but the spherical end of the cylindrical precipitate is clearly visible in the HRTEM image. It is likely that the complexity of the FFT spectra in Fig. 5 is associated with the combination of two θ' phases nucleated on one cylindrical precipitate. As described earlier, the abnormally thick θ' phase may not follow the typical orientation relationship with the matrix. Interestingly the heterogeneous nucleation of plate type of

Al_2Cu phase (Ω phase) has been reported to occur upon the various second phases in the Al-Cu-Mg-Ag baseline alloys (Ringer et al., 1996).

Hirosawa et al. (2000) reported a Si microalloying effect on the increase in number density of Mg/Cu/vacancy complexes resulting in finer and denser rod-type GPB zones. They found that these GPB zones stimulated intragranular precipitation of the hardening Ω phase. Interestingly, the cylindrical precipitates observed in this study were served as heterogeneous nucleation sites for the θ' phase as well as a dominant hardening phase even for high aging temperatures. The association of Mg-Cu clusters with Si during the early stages of precipitation, i.e., the cylindrical precipitate, serves to preferentially nucleate θ' phase instead of the Ω phase. However, the presence of two apparently different types of heterogeneous nucleation needs to be resolved as understanding and controlling it may allow an increase in the density of the θ' phase and significantly enhance the mechanical properties of quaternary Al-Si-Cu-Mg alloys as compared to the Si free Al-Cu-Mg alloys.

CONCLUSIONS

Two different types of θ' particles were introduced in the low-Si aluminum casting alloys. These appear to nucleate heterogeneously and grow in a manner not previously reported. The morphologies of these θ' precipitates are definitely influenced by the nature of their nucleation sites, which also affect the density of hardening precipitates.

ACKNOWLEDGMENTS

The authors gratefully acknowledge the Center for Advanced Research and Technology (CART) at the University of North Texas for the use of facilities and the Korea Institute of Science and Technology (KIST) Institutional Program in Republic of Korea.

REFERENCES

Eskin D G (2003) Decomposition of supersaturated solid solutions in Al–Cu–Mg–Si alloys. *J. Mater. Sci*. **38**, 279-290.

Fujita H C and Lu C (1992) An electron microscope study of G.P. zones and θ' – phase in Al-1.6 at % Cu crystals. *Mater. Trans. JIM* **33**, 892-896.

Guinier A (1938) Structure of age-hardened aluminium-copper alloys. *Nature* **142**, 569-570.

Hirosawa S, Sato T, Kamio A, and Flower H M (2000) Classification of the role of microalloying elements in phase decomposition of Al based alloys. *Acta Mater*. **48**, 1797-1806.

Hono K, Sano N, Babu S S, Okano R, and Sakurai T (1993) Atom probe study of the precipitation process in Al-Cu-Mg-Ag alloys. *Acta Metall. Mater*. **41**, 829-838.

Hutchinson C R and Ringer S P (2000) Precipitation processes in Al-Cu-Mg alloys microalloyed with Si. *Metall. Mater. Trans*. **31A**, 2721-2733.

Hwang J Y, Banerjee R, Doty H W, and Kaufman M J (2009) The effect of Mg on the structure and properties of type 319 aluminum casting alloys. *Acta Mater*. **57**, 1308-1317.

Konno T J, Hiraga K, and Kawasaki M (2001) Guinier-preston (GP) zone revisited: atomic level observation by HAADF-TEM technique. *Scripta Mater*. **44**, 2303-2307.

Martin J W (1980) *Micromechanism in Particle-hardened Alloys* (Cambridge University Press, Cambridge).

Miller M K and Russell K F (2007) Atom probe specimen preparation with a dual beam SEM/FIB miller. *Ultramicroscopy* **107**, 761-766.

Mukhopadhyay (2002) Coprecipitation of Ω and σ phases in Al-Cu-Mg-Mn alloys containing Ag and Si. *Metall. Mater. Trans*. **33A**, 3635-3648.

Preston G P (1938) Structure of age-hardened aluminium-copper alloys. *Nature* **142**, 570.

Ringer S P, Hono K, Polmear I J, and Sakurai T (1996) Nucleation of precipitates in aged Al-Cu-Mg-(Ag) alloys with high Cu:Mg ratios. *Acta Mater*. **44**, 1883-1898.

Thompson K, Lawrence D, Larson D J, Olson J D, Kelly T F, and Gorman B (2007) In situ site-specific specimen preparation for atom probe tomography. *Ultramicroscopy* **107**, 131-139.